Cell Reports

Autophagy Controls CSL/RBPJκ Stability through a p62/SQSTM1-Dependent Mechanism

Graphical Abstract

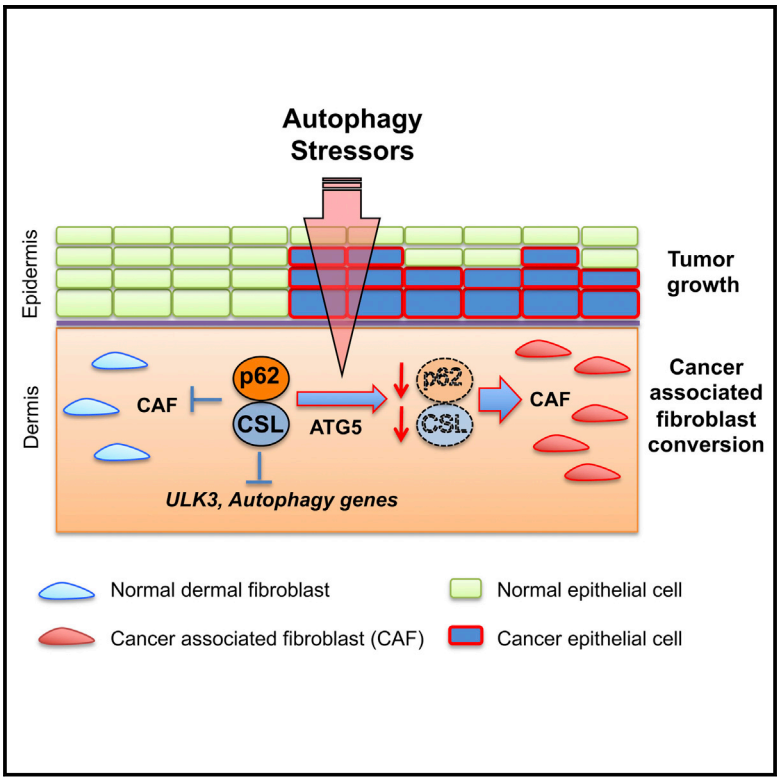

Highlights

- Autophagy down-modulates CSL/RBPJk in stromal fibroblasts
- CSL degradation by autophagy requires interaction with p62 adaptor
- CSL down-modulation by autophagy induces cancer-associated fibroblast (CAF) genes
- CSL overexpression in CAFs stabilizes p62 and represses expression of autophagy genes

Authors

Sandro Goruppi, Seung-Hee Jo, Csaba Laszlo, Andrea Clocchiatti, Victor Neel, G. Paolo Dotto

Correspondence

paolo.dotto@unil.ch

In Brief

Autophagic conditions are often found in the tumor stroma, where CSL/RBPJκ levels are down-modulated. Goruppi et al. identify a key role for autophagy in the degradation of CSL through a direct interaction with the p62 adaptor. This induces CSL-repressed genes involved in CAF activation and autophagy, linking the two processes.

Goruppi et al., 2018, Cell Reports *24*, 3108–3114
September 18, 2018
https://doi.org/10.1016/j.celrep.2018.08.043

CellPress

OPEN ACCESS
CellPress

Cell Reports
Report

Autophagy Controls CSL/RBPJκ Stability through a p62/SQSTM1-Dependent Mechanism

Sandro Goruppi,[1,2] Seung-Hee Jo,[1,2] Csaba Laszlo,[3] Andrea Clocchiatti,[1,2] Victor Neel,[4] and G. Paolo Dotto[1,3,5,*]
[1]Cutaneous Biology Research Center, Massachusetts General Hospital, 149 Bldg. 13th St. Charlestown, MA 02129, USA
[2]Department of Dermatology, Harvard Medical School, Boston, MA 02125, USA
[3]Department of Biochemistry, University of Lausanne, 155 Chemin des Boveresses, Epalinges 1066, Switzerland
[4]Department of Dermatology, Massachusetts General Hospital, Boston, MA 02114, USA
[5]Lead Contact
*Correspondence: paolo.dotto@unil.ch
https://doi.org/10.1016/j.celrep.2018.08.043

SUMMARY

Cancer-associated fibroblasts (CAFs) are important at all tumor stages. CSL/RBPJκ suppresses the gene expression program leading to CAF activation and associated metabolic reprogramming, as well as autophagy. Little is known about CSL protein turnover, especially in the tumor microenvironment. We report that, in human dermal fibroblasts (HDFs), conditions inducing autophagy—often found in tumor stroma—down-regulate CSL protein levels but do not affect its mRNA levels. Genetic or pharmacologic targeting of the autophagic machinery blocks CSL down-modulation. Mechanistically, endogenous CSL associates with the autophagy and signaling adaptor p62/SQSTM1, which is required for CSL down-modulation by autophagy. This is functionally significant, because both CSL and p62 levels are lower in skin cancer-derived CAFs, in which autophagy is increased. Increasing cellular CSL levels stabilizes p62 and down-modulates the autophagic process. We reveal here an autophagy-initiated mechanism for CSL down-modulation, which could be targeted for stroma-focused cancer prevention and treatment.

INTRODUCTION

Autophagy is a homeostatic metabolic mechanism responsible for bulk degradation of cellular molecules and organelles (Levine and Kroemer, 2008; Mizushima and Komatsu, 2011). Although key for cancer initiation and progression (White, 2015), the involvement of autophagy in the stromal compartment, and in particular in cancer-associated fibroblast (CAF) activation, has been investigated to a limited extent. Autophagy-activating conditions, such as low nutrients, increased reactive oxygen species (ROS) (Pavlides et al., 2010), and hypoxia (Martinez-Outschoorn et al., 2010), are often found in cancer stroma (Zhao et al., 2013). In this context, a reverse Warburg effect concept was introduced, whereby activation of stromal autophagy and mitophagy by hypoxia (Martinez-Outschoorn et al., 2010), senescence (Capparelli et al., 2012a), and autophagy effectors (Capparelli et al., 2012b) leads to a glycolytic switch producing high-energy intermediates, such as ketones and lactate, which impinge on cancer cells promoting tumor growth and metastasis (Martinez-Outschoorn et al., 2011, 2017).

The CSL/RBPJκ (CSL) protein, a transcriptional repressor converted by NOTCH into an activator, is key for negative control of CAF activation. Deletion of *Csl* in the mesenchymal skin compartment of mice or *CSL* down-modulation in primary human dermal fibroblasts (HDFs) results in the activation of a CAF phenotype (Hu et al., 2012; Procopio et al., 2015). We have shown that CSL loss in HDFs leads to up-regulation of the pro-autophagy kinase ULK3, which is responsible for CAF activation and concomitantly activates autophagy and a mitophagy-associated glycolytic switch (Goruppi et al., 2017).

The adaptor protein sequestosome 1 (p62/SQSTM1) plays a key role in the autophagic process, functioning as cargo for specific proteins, including key transcription factors like SMADs and nuclear factor κB (NF-κB), to be degraded in autophagosomes, with p62 being degraded in the process (Moscat and Diaz-Meco, 2009). p62 is down-regulated in the stroma of several cancer types, and its down-modulation has been implicated in the metabolic reprogramming of stromal CAFs through an mTORC1/Myc pathway regulating interleukin-6 (IL-6) production (Valencia et al., 2014). In the liver, loss of p62 activates stromal stellate cells, resulting in higher inflammation and fibrosis due to impaired vitamin D receptor (VDR) signaling with p62 functioning in this context as a transcriptional co-regulator (Duran et al., 2016). Little is known about the control of CSL protein turnover, particularly in the tumor microenvironment. We report here a so far unsuspected interplay between p62 and CSL. p62 and CSL proteins associate physically, and upon induction of autophagy, CSL is down-modulated in stromal fibroblasts through a p62-dependent mechanism. This is functionally significant, because CSL and p62 are concomitantly down-modulated in clinically derived CAFs and increased CSL stabilizes p62, decreasing the expression of autophagic genes.

RESULTS

Loss of Csl repressive function in mouse dermal fibroblasts and HDFs leads to CAF activation (Hu et al., 2012; Procopio et al., 2015). Concomitantly, we showed that *CSL* down-modulation

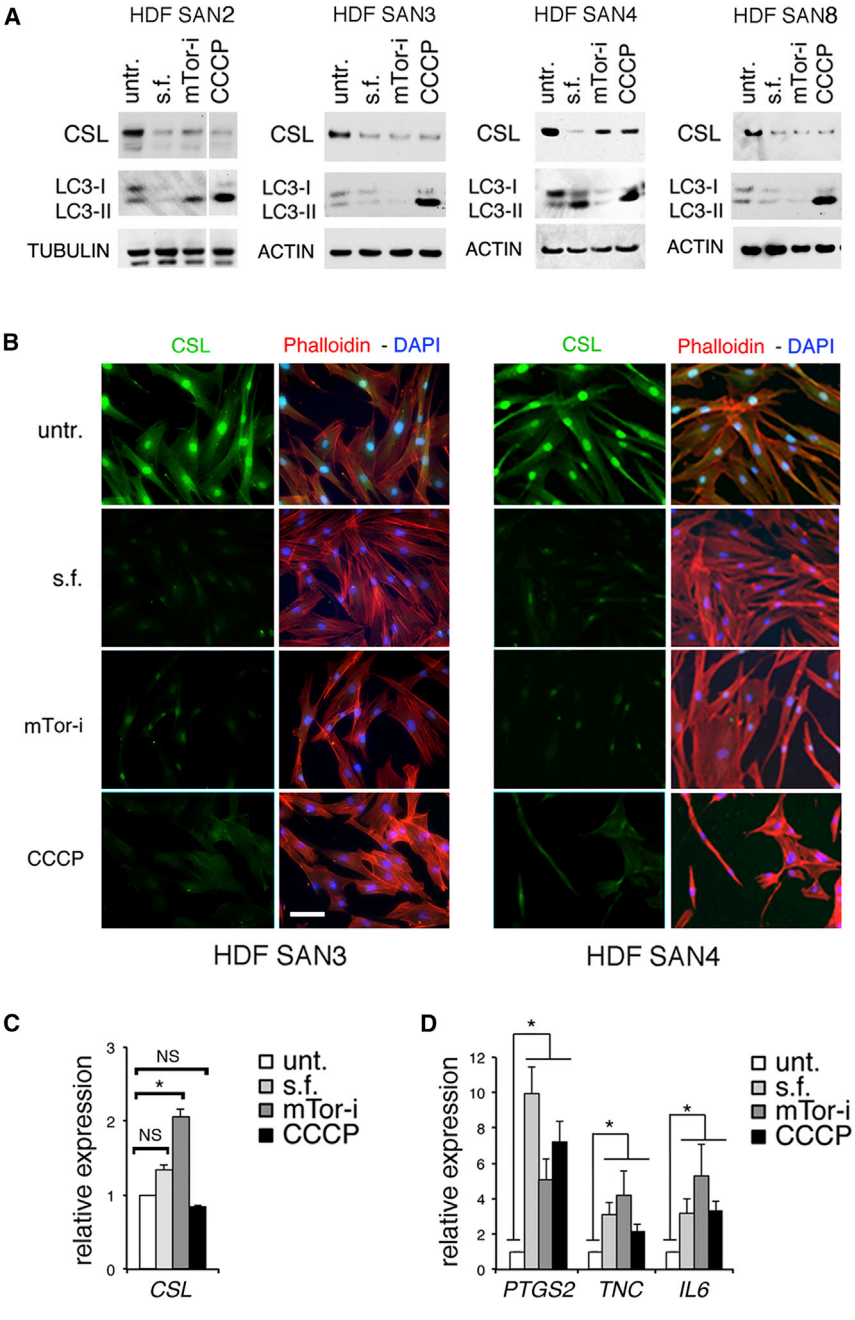

Figure 1. Autophagy Down-Modulates CSL Protein

(A) CSL is down-regulated by autophagy. Immunoblot analysis was performed for four HDF strains that were untreated (untr.), serum starved (s.f.), or treated with the KU0063794 mTOR inhibitor (mTOR-i; 10 μM) or a mitochondria-uncoupling agent (CCCP; 5 μM) for 24 hr to induce autophagy. Blots were sequentially probed with antibodies against CSL, LC3- to monitor autophagic processing, and with anti γ-Tubulin (TUBULIN) or β-Actin (ACTIN), as equal loading. The identifier of the operator and a progressive number classify each primary HDF strain (e.g., SAN3), and a list of all the cells used is provided in Key Resources Table.

(B) Immunofluorescence analysis with anti-CSL antibodies (green), phalloidin (red), and DAPI (blue) of two HDF strains treated as in (A). Phalloidin and DAPI counterstained the cytoskeleton and the nuclei, respectively. Scale bar, 40 μm.

(C) Autophagy down-modulates CSL protein independently of its RNA levels. RT-qPCR analysis of *CSL* expression, normalized to *β-actin*, of two HDF strains (SAN4 and SAN5) treated as in (A).

(D) CSL down-modulation results in the upregulation of CAF effector genes. RT-qPCR analysis of the indicated CAF effector gene expression, normalized to *β-actin*, of two HDF (SAN2 and SAN3) treated as in (A).

Mean ± SEM; n (experiments) = 3; NS, not significant; *p ≤ 0.05, two-tailed unpaired t test.

and immunoblotting (Figures 1A and 1B). Decreased CSL protein levels are not a secondary consequence of reduced transcription, because *CSL* mRNA was not concomitantly down-modulated after these treatments (Figure 1C), and they are functionally significant, because we observed a simultaneous upregulation of CAF effector genes such as cyclooxygenase-2 (*PTGS2*), tenascin-C (*TNC*), and *IL6* (Figure 1D).

To assess whether CSL protein down-modulation is a consequence of increased autophagy, we employed several complementary approaches. 3-methyladenine (3MA) blocks early steps of the autophagic process by targeting type III phosphatidylinositol 3-kinases (Klionsky et al., 2016). Treatment of HDFs with this inhibitor counteracted the down-modulation of CSL by various inducers of autophagy while resulting in an accumulation of p62/SQSTM1 (p62), a cargo protein that is degraded by autophagic flux (Klionsky et al., 2016) (Figure 2A). As a more specific approach, we targeted the *ATG5* gene, which is essential for autophagosome elongation (Klionsky et al., 2016; Kuma et al., 2004). Down-modulation of the CSL protein by the various inducers of autophagy was suppressed in HDFs with small hairpin RNA (shRNA)-mediated down-modulation of *ATG5*, as well as in mouse embryo fibroblasts (MEFs) with *Atg5* gene disruption

increases HDF autophagy, mitophagy, and associated metabolic reprogramming (Goruppi et al., 2017). Previous evidence reported that pro-carcinogenic stimuli such as ultraviolet A rays (UVAs) and smoke extract exposure, which induce autophagy (Ratovitski, 2011; Sample et al., 2017), similarly down-regulate CSL (Menietti et al., 2016). Using specific experimental conditions activating different types of autophagy, we determined that all inducers of autophagy affected CSL protein levels. Conditions such as serum starvation, inhibition of mTOR activity, and mitochondria uncoupling down-regulated CSL protein levels in HDFs, as seen by immunofluorescence

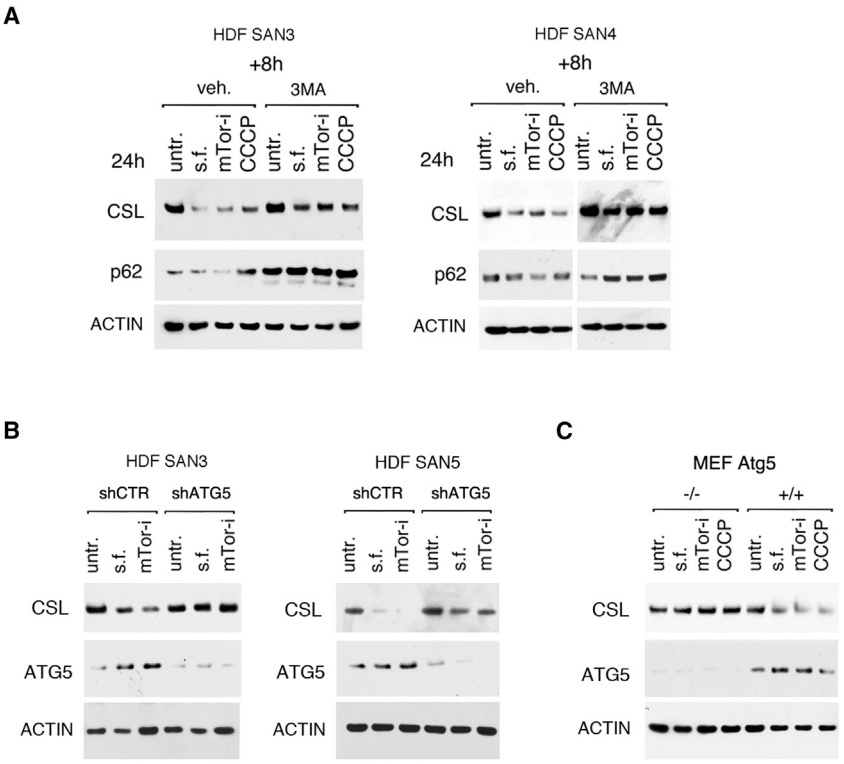

Figure 2. CSL Protein Down-Modulation Requires Autophagy

(A) Pharmacologic inhibition of autophagy blocks CSL down-modulation. Immunoblot analysis was performed for two HDF strains treated as indicated in Figure 1A for 24 hr and further incubated with 5 mM 3-methyladenine (3MA) for 8 hr to inhibit autophagy, in parallel with vehicle alone (DMEM). The blot was sequentially probed with antibodies against CSL, p62, and β-ACTIN.

(B and C) Targeting of autophagy-essential gene *ATG5* blocks CSL down-modulation. Immunoblot analysis was performed for two HDFs plus/minus shRNA-mediated *ATG5* gene silencing (B) or for mouse embryo fibroblasts (MEFs) plus/minus *Atg5* gene disruption (+/+ and −/−) (Kuma et al., 2004) (C) that were either left untreated (untr.) or treated with various pro-autophagic stimuli as in Figure 1A. Blots were sequentially probed with antibodies against CSL, ATG5, and ACTIN as equal loading.

(Figures 2B and 2C). Thus, pro-autophagic stimuli down-modulate CSL protein levels through a mechanism requiring the autophagic machinery.

p62 has a cargo function for several transcription factors (Johansen and Lamark, 2011; Katsuragi et al., 2015), and an attractive possibility was that it physically associates with CSL. Proximity ligation assays (PLAs) provide a sensitive method for detection of protein-protein associations at the cellular level (Söderberg et al., 2006). We found punctate signals (*puncta*) resulting from the juxtaposition of anti-CSL and anti-p62 antibodies in HDFs (Figures 3A and S1A), with the number of these *puncta* being significantly reduced by *CSL* silencing as a specificity control (Figures 3B and S1B). More directly, we found that endogenous p62 and CSL were recovered by co-immunoprecipitation from HDFs (Figures 3C and S1C). Similar positive results were obtained after co-immunoprecipitation of the two recombinant proteins, demonstrating a direct interaction between the two (Figure 3D).

The p62 protein contains several functional regions, including an N-terminal oligomerization domain (protein homo/hetero dimerization domain of p62 [PB1]), a light-chain 3 (LC3)-interacting region (LIR), and a C-terminal ubiquitin-association (UBA) domain (Johansen and Lamark, 2011; Moscat and Diaz-Meco, 2009). Co-immunoprecipitation experiments of HEK293 cells co-transfected with expression vectors for CSL, together with p62 deletion mutants disrupting these various regions (Bjørkøy et al., 2005), showed that binding of CSL was unaffected by all p62 mutations except the one with a deletion of the 50 amino acid C-terminal domain, more directly implicated in the delivery of proteins to degradation (Johansen and Lamark, 2011; Komatsu et al., 2007) (Figure 3E).

To assess whether CSL-p62 interaction is of functional importance for CSL degradation, we tested whether p62 is required for CSL down-modulation by autophagy stressors. We found that down-modulation of CSL protein levels by autophagy stressors was suppressed in both HDFs or MEFs with small interfering RNA (siRNA)- or shRNA-mediated *p62* silencing (Figures 4A and 4B). Similarly, CSL down-modulation by autophagy stressors was blocked in MEFs with *p62* gene disruption (Figures 4C and 4D). The preceding findings are of likely clinical significance for HDF to CAF activation, in which we showed that CSL down-modulation induces autophagy (Goruppi et al., 2017). Immunoblot analysis showed parallel down-modulation of CSL and p62 levels in a set of skin squamous cell carcinoma (SCC)-derived CAF strains versus non-matched HDFs (Figure 5A).

Functionally, increased CSL expression by lentiviral vector infection of HDFs resulted in concomitantly enhanced p62 levels under basal conditions and after autophagy activation by serum starvation, in both the presence and the absence of bafilomycin A1, which prevents lysosomal acidification step of the autophagic flux (Figure 5B). On this line, we found that *CSL* overexpression was paralleled by the suppression of three autophagy marker genes (Figure 5C) that we have shown to be up-regulated by CSL loss in HDFs (Goruppi et al., 2017).

Decreased p62 is causative to CAF activation in multiple systems (Duran et al., 2016; Valencia et al., 2014). We found that *CSL* overexpression in patient-derived CAFs similarly stabilized the levels of p62 (Figure 5D), consistent with the reversion of CAF phenotype after *CSL* overexpression (Procopio et al., 2015).

CSL protein expression is negatively controlled by autophagy through a mechanism involving a direct CSL-p62 protein association. In turn, by decreasing the autophagic process, CSL functions as a positive determinant of p62 expression levels, pointing

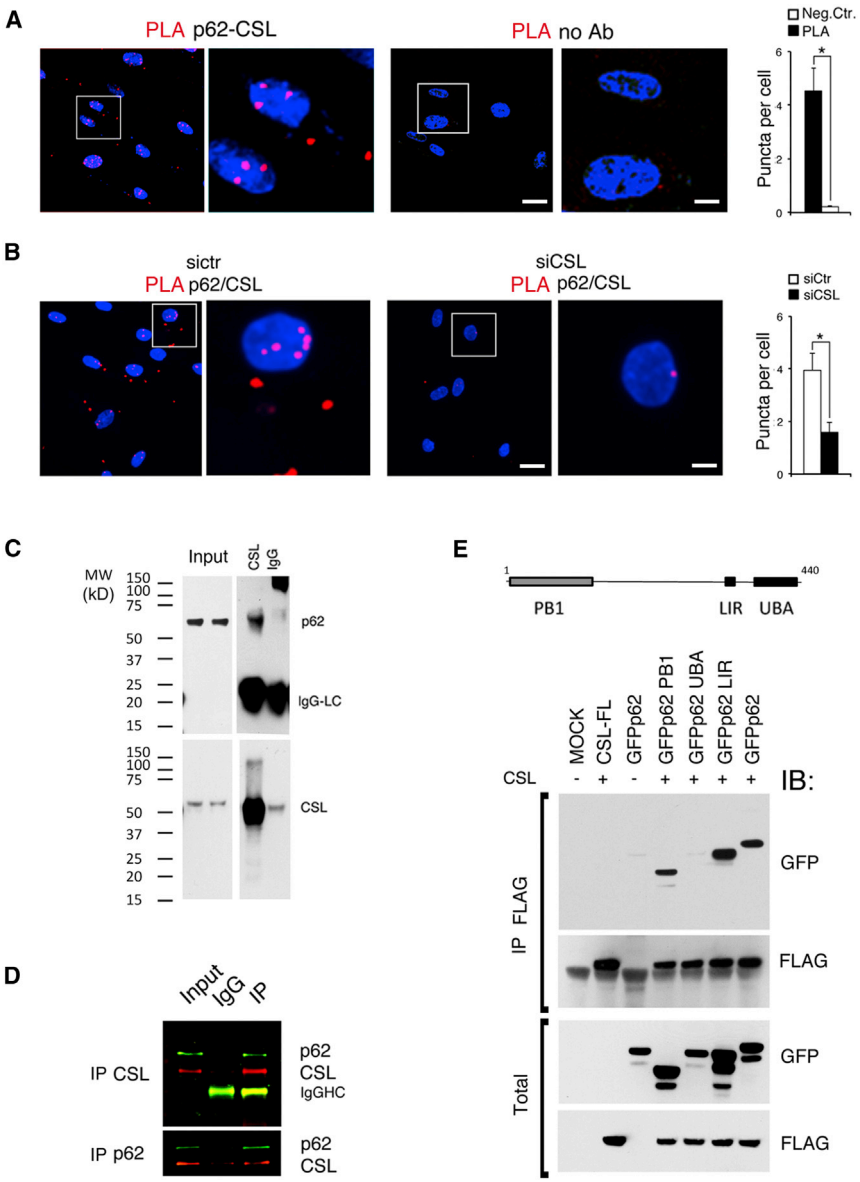

Figure 3. Endogenous p62 and CSL Proteins Directly Interact in HDFs

(A and B) Proximity ligation assays (PLAs) for *in situ* detection of CSL and p62 association in HDFs. Assays were carried out in the presence or absence of primary antibodies (A) or with HDFs plus/minus siRNA-mediated *CSL* gene silencing (B) as controls of specificity. Confocal microscopy was used to examine red fluorescence PLA *puncta* with concomitant DAPI staining of nuclei (blue). The white frames indicate the enlarged areas to better show PLA red *puncta*. Shown are representative images and quantification of the average number of *puncta* per cell, counting at least 30 cells in four fields per conditions. $p \leq 0.05$, two-tailed unpaired t test. Scale bars, 10 and 1 μm for enlargements. Additional PLA images of p62 and CSL interaction are provided in Figures S1A and S1B.

(C) Endogenous p62 and CSL proteins interact. Immunoprecipitates from HDFs (strain SAN4) with anti-CSL antibodies and non-immune immunoglobulin Gs (IgGs) were analyzed, together with total inputs by sequential immunoblotting with anti-p62 and CSL antibodies. IgG light chains (LCs) are indicated. A similar immunoprecipitation in another HDF strain (SAN3) is shown in Figure S1C.

(D) p62 and CSL proteins directly interact. Recombinant CSL and p62 proteins were admixed and incubated for 2 hr before immunoprecipitation with either anti-CSL or anti-p62 antibodies or non-immune IgGs, followed by immunoblot analysis with anti-p62 antibodies (green) and anti-CSL antibodies (red). IgG heavy chains (HCs) are indicated.

(E) p62 interaction with CSL requires p62 C-terminal region. Immunoblot analysis showed HEK293 transfected for 48 hr with expression vectors for CSL-FLAG, GFP-p62, and a combination of CSL-FLAG and GFP-p62 wild-type (WT) or GFP-p62 constructs with deletions of the N-terminal PB1 region, LIR, and C-terminal UBA region (as indicated in the scheme) (Bjørkøy et al., 2005). Total lysates were immunoprecipitated with anti-FLAG antibodies, and blots were probed sequentially with anti-GFP and anti-FLAG antibodies. The input totals were analyzed by parallel immunoblotting as control for the level of expression.

to a self-reinforcing loop that could be targeted in CAF activation.

DISCUSSION

In tumor stroma, CAFs affect all aspects of tumor evolution (Dotto, 2014; Kalluri, 2016). Thus, targeting of CAFs represents an emerging alternative therapeutic approach (Goruppi and Dotto, 2013). Although several programs leading to the activation of CAFs have been elucidated, little is known about the impact of the microenvironment on the turnover of key CAF regulators. CSL, a transcriptional repressor that mediates NOTCH signaling, suppresses the gene expression programs, leading to stromal senescence and CAF activation (Hu et al., 2012; Procopio et al., 2015). We report here that increased autophagy increases CSL turnover, which is functionally relevant, because it is associated with enhanced CAF effector expression. We find a so far unsuspected interplay between CSL and p62 signaling leading to CAF activation. p62 and CSL proteins associate directly, and upon induction of autophagy, CSL is down-modulated in stromal fibroblasts through a p62-dependent mechanism. In CAFs, both CSL and p62 proteins are down-modulated as a reflection of increased autophagy in these cells (Goruppi et al., 2017).

Autophagy-enhancing conditions, such as ROS (Pavlides et al., 2010), hypoxia (Martinez-Outschoorn et al., 2010), and nutrient starvation (Martinez-Outschoorn et al., 2017), can create a pro-tumorigenic microenvironment rich in metabolic precursors

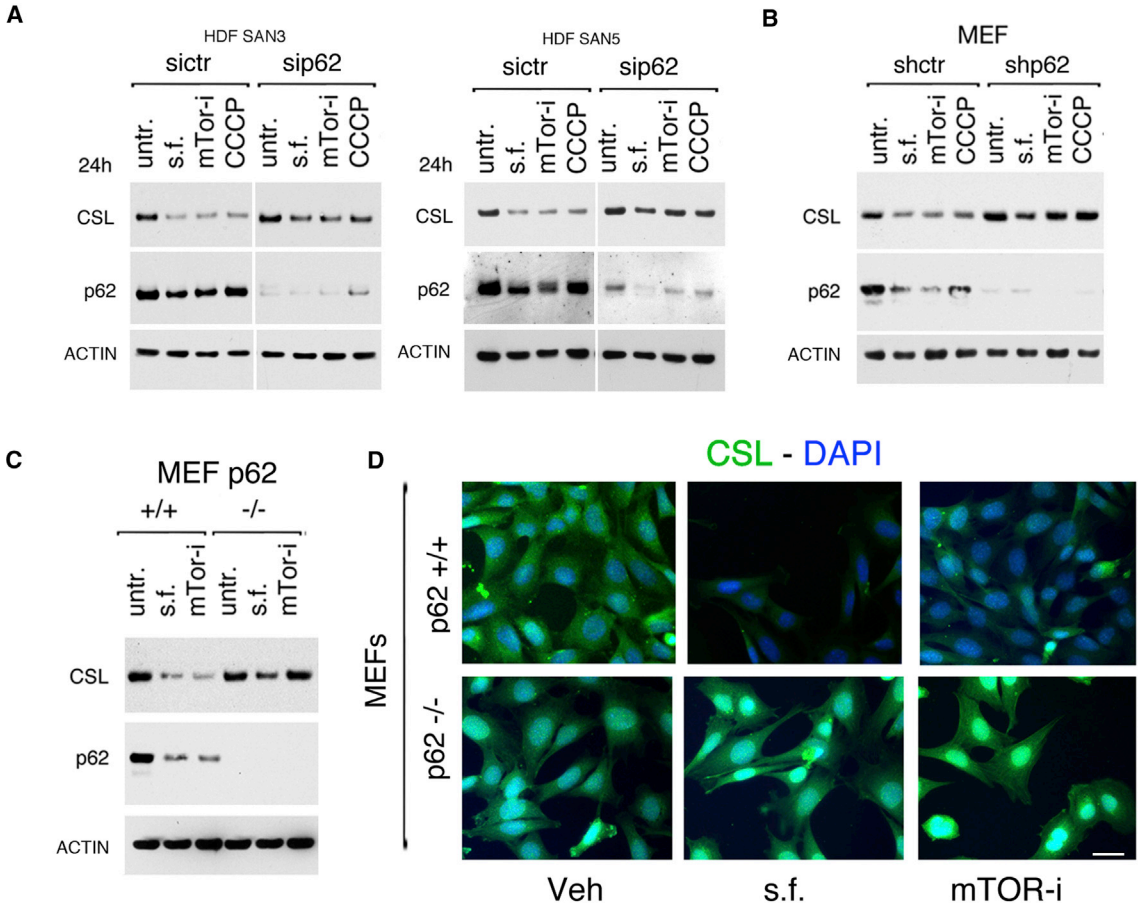

Figure 4. Autophagy Down-Modulates CSL Protein through a p62-Dependent Mechanism

(A and B) Immunoblot analysis of two HDF strains (A) or MEFs (B) plus/minus *p62* silencing by siRNA-mediated (A) or shRNA-mediated (B) RNA interference, either left untreated (untr.) or treated with various pro-autophagic stimuli as in Figure 1A. Blots were sequentially probed with antibodies against p62, CSL, and ACTIN antibodies.

(C) Immunoblot analysis with antibodies against p62, CSL, and ACTIN antibodies of MEFs plus/minus p62 gene disruption (−/− and +/+) (Komatsu et al., 2006). Cells were either left untreated (untr.) or treated with various pro-autophagic stimuli as in Figure 1A.

(D) Immunofluorescence analysis with CSL antibodies and DAPI of *p62* +/+ and *p62* −/− MEFs treated as in Figure 1A.

directed from the stroma to the tumor (Lisanti et al., 2010; Zhao et al., 2013). As for CSL (Hu et al., 2012; Procopio et al., 2015), p62 protein and RNA levels are reduced in the stromal compartment of several cancer types, with p62 deficiency, resulting in CAF activation (Valencia et al., 2014). An unanswered question was whether CSL and p62 are functionally connected. p62 is a multifaceted adaptor protein involved in functions ranging from nutrient or amino acid sensing and oxidative stress response to selective autophagy (Katsuragi et al., 2015). The cargo function of this protein is mediated by its ubiquitin-association (UBA) domain, which is involved in target protein recognition, and by its LIR, required for autophagosome recruitment and degradation. p62 binds to key transcription factors like SMADs, NRF2, and NF-κB to be degraded in autophagosome, with p62 being degraded in the process (Johansen and Lamark, 2011). We have found that CSL is down-modulated by autophagy, because genetic or pharmacologic inhibition of the process blunts CSL degradation. Upon autophagy activation, the mechanism involves the physical and direct association to the UBA domain of p62 adaptor. Another protein with key transcription regulatory functions, GATA4, was shown to similarly go through autophagic turnover mediated by p62 binding (Kang et al., 2015).

Transcriptional control of autophagy is an area of active investigation (Lapierre et al., 2015; Pietrocola et al., 2013) and autophagy and mitophagy have been implicated in CAF conversion (Goruppi et al., 2017; Kalluri, 2016; Martinez-Outschoorn et al., 2017). Besides being negatively regulated by autophagy, down-modulation of CSL expression—as can result from exogenous pro-carcinogenic stimuli such as UV or smoke exposure (Menietti et al., 2016)—can by itself induce or re-enforce the autophagic process (Goruppi et al., 2017). An interesting possibility is that autophagy acts at multiple levels in CAF activation, initiating gene expression by increasing CSL turnover and by causing a cell-autonomous metabolic switch upon the increase of autophagy and mitophagy after CSL

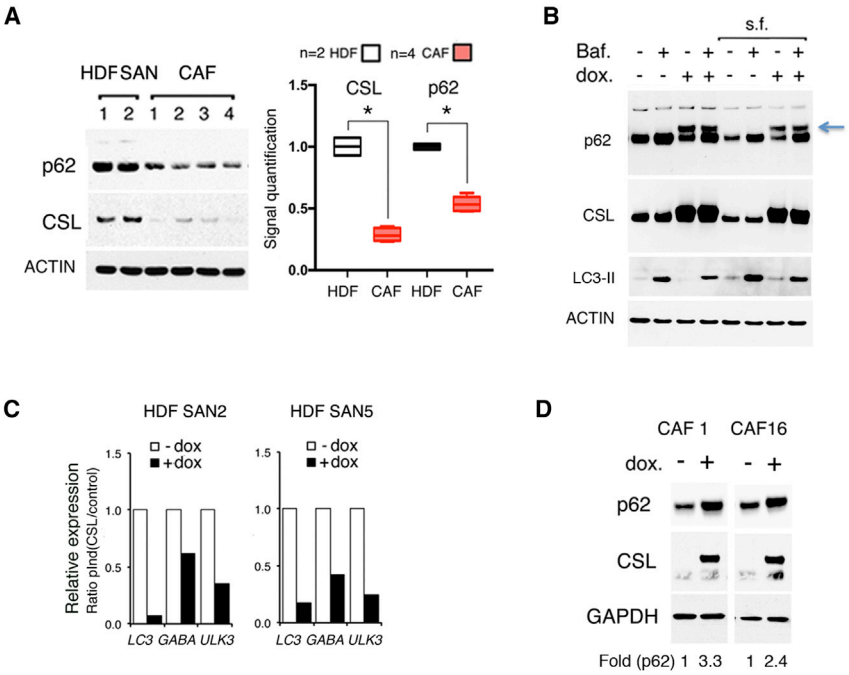

Figure 5. CSL Down-Modulation Is Linked to Higher Autophagy in CAFs

(A) p62 and CSL levels are concomitantly down-modulated in CAFs. Left: immunoblot with anti-p62, anti-CSL, and anti-ACTIN antibodies in non-matched HDF and CAF strains. Right: immunoblot quantifications, n (HDF) = 2, n (CAF) = 4; *p < 0.05, two-tailed unpaired t test. Each derived HDF strain was marked by an operator identifier and progressive numbers (SAN1 and SAN2). CAF strains were marked only by a progressive number (CAF1–CAF4) (Goruppi et al., 2017).

(B) *CSL* overexpression stabilizes p62 protein. Immunoblot analysis showed HDFs (SAN3) stably infected with a lentivirus for doxycycline-inducible CSL expression (Procopio et al., 2015), plus/minus doxycycline (200 ng/mL) for 3 days, under basal conditions and after autophagy activation by serum starvation (24 hr). Bafilomycin A1 was added for 2 hr to monitor autophagic flux (Klionsky et al., 2016). The arrow indicates the stabilized high-molecular p62 band upon CSL induction. The blots were sequentially probed with antibodies against p62, LC3, CSL, and ACTIN.

(C) CSL overexpression inhibits autophagy gene expression. RT-qPCR analysis with the indicated genes, normalized to *β-actin*, in two HDF strains stably infected with an inducible *CSL*-expressing lentivirus, plus/minus CSL induction as in (B).

(D) *CSL* overexpression stabilizes p62 in CAFs. Immunoblot analysis showed antibodies against p62, CSL, and GAPDH of two patient-derived CAF strains (CAF1 and CAF16) expressing a doxycycline-inducible CSL and plus/minus (200 ng/mL) for 2 days.

Numbers refer to densitometry quantification of p62 in *CSL*-overexpressing versus noninduced control CAFs (folds of induction).

loss of function (Goruppi et al., 2017). Counteracting CSL down-modulation can stabilize p62, thereby enhancing the nuclear transcription regulatory function that this protein plays in negative control of CAF activation (Duran et al., 2016; Valencia et al., 2014).

STAR★METHODS

Detailed methods are provided in the online version of this paper and include the following:

- KEY RESOURCES TABLE
- CONTACT FOR REAGENT AND RESOURCE SHARING
- EXPERIMENTAL MODEL AND SUBJECT DETAILS
  - Human samples
  - Cell culture and primary cell derivation
- METHOD DETAILS
  - Cell manipulation
  - Gene Expression analysis
  - Autophagy studies, immunofluorescence and immunoblots
  - Immunoprecipitations and protein interaction
- QUANTIFICATION AND STATISTICAL ANALYSIS
- DATA AND SOFTWARE AVAILABILITY

SUPPLEMENTAL INFORMATION

Supplemental Information includes one figure and one table and can be found with this article online at https://doi.org/10.1016/j.celrep.2018.08.043.

ACKNOWLEDGMENTS

We thank Masaaki Komatsu, Toru Yanagawa, and Noburo Mitzushima for providing the *Atg5* and *p62* −/− and +/+ MEFs. We are grateful to Terje Johanssen for providing the GFP-p62 constructs and Alessia Di Nardo for the ATG5- and p62-targeting shRNAs. The work was supported by grants from the NIH (R01AR039190 and R01AR064786; the content does not necessarily represent the official views of the NIH), the Swiss National Science Foundation "Genomic instability and evolution in cancer stromal cells" (310030B_176404), and the European Research Council (26075083) to G.P.D.

AUTHOR CONTRIBUTIONS

S.G., S.J., C.L., and A.C. performed the experiments and contributed to analysis of the results. V.N. provided clinical samples. S.G. and G.P.D. designed the study. S.G. and G.P.D. wrote the manuscript.

DECLARATION OF INTERESTS

The authors declare no competing interests.

Received: February 1, 2018
Revised: July 9, 2018
Accepted: August 15, 2018
Published: September 18, 2018

REFERENCES

Bjørkøy, G., Lamark, T., Brech, A., Outzen, H., Perander, M., Overvatn, A., Stenmark, H., and Johansen, T. (2005). p62/SQSTM1 forms protein aggregates degraded by autophagy and has a protective effect on huntingtin-induced cell death. J. Cell Biol. *171*, 603–614.

Capparelli, C., Chiavarina, B., Whitaker-Menezes, D., Pestell, T.G., Pestell, R.G., Hulit, J., Andò, S., Howell, A., Martinez-Outschoorn, U.E., Sotgia, F., and Lisanti, M.P. (2012a). CDK inhibitors (p16/p19/p21) induce senescence and autophagy in cancer-associated fibroblasts, "fueling" tumor growth via paracrine interactions, without an increase in neo-angiogenesis. Cell Cycle *11*, 3599–3610.

Capparelli, C., Guido, C., Whitaker-Menezes, D., Bonuccelli, G., Balliet, R., Pestell, T.G., Goldberg, A.F., Pestell, R.G., Howell, A., Sneddon, S., et al. (2012b). Autophagy and senescence in cancer-associated fibroblasts metabolically supports tumor growth and metastasis via glycolysis and ketone production. Cell Cycle *11*, 2285–2302.

Dotto, G.P. (2014). Multifocal epithelial tumors and field cancerization: stroma as a primary determinant. J. Clin. Invest. *124*, 1446–1453.

Duran, A., Hernandez, E.D., Reina-Campos, M., Castilla, E.A., Subramaniam, S., Raghunandan, S., Roberts, L.R., Kisseleva, T., Karin, M., Diaz-Meco, M.T., and Moscat, J. (2016). p62/SQSTM1 by binding to vitamin D receptor inhibits hepatic stellate cell activity, fibrosis, and liver cancer. Cancer Cell *30*, 595–609.

Goruppi, S., and Dotto, G.P. (2013). Mesenchymal stroma: primary determinant and therapeutic target for epithelial cancer. Trends Cell Biol. *23*, 593–602.

Goruppi, S., Procopio, M.G., Jo, S., Clocchiatti, A., Neel, V., and Dotto, G.P. (2017). The ULK3 kinase is critical for convergent control of cancer-associated fibroblast activation by CSL and GLI. Cell Rep. *20*, 2468–2479.

Hu, B., Castillo, E., Harewood, L., Ostano, P., Reymond, A., Dummer, R., Raffoul, W., Hoetzenecker, W., Hofbauer, G.F., and Dotto, G.P. (2012). Multifocal epithelial tumors and field cancerization from loss of mesenchymal CSL signaling. Cell *149*, 1207–1220.

Johansen, T., and Lamark, T. (2011). Selective autophagy mediated by autophagic adapter proteins. Autophagy *7*, 279–296.

Kalluri, R. (2016). The biology and function of fibroblasts in cancer. Nat. Rev. Cancer *16*, 582–598.

Kang, C., Xu, Q., Martin, T.D., Li, M.Z., Demaria, M., Aron, L., Lu, T., Yankner, B.A., Campisi, J., and Elledge, S.J. (2015). The DNA damage response induces inflammation and senescence by inhibiting autophagy of GATA4. Science *349*, aaa5612.

Katsuragi, Y., Ichimura, Y., and Komatsu, M. (2015). p62/SQSTM1 functions as a signaling hub and an autophagy adaptor. FEBS J. *282*, 4672–4678.

Klionsky, D.J., Abdelmohsen, K., Abe, A., Abedin, M.J., Abeliovich, H., Acevedo Arozena, A., Adachi, H., Adams, C.M., Adams, P.D., Adeli, K., et al. (2016). Guidelines for the use and interpretation of assays for monitoring autophagy (3rd edition). Autophagy *12*, 1–222.

Komatsu, M., Waguri, S., Chiba, T., Murata, S., Iwata, J., Tanida, I., Ueno, T., Koike, M., Uchiyama, Y., Kominami, E., and Tanaka, K. (2006). Loss of autophagy in the central nervous system causes neurodegeneration in mice. Nature *441*, 880–884.

Komatsu, M., Waguri, S., Koike, M., Sou, Y.S., Ueno, T., Hara, T., Mizushima, N., Iwata, J., Ezaki, J., Murata, S., et al. (2007). Homeostatic levels of p62 control cytoplasmic inclusion body formation in autophagy-deficient mice. Cell *131*, 1149–1163.

Kong, D.K., Georgescu, S.P., Cano, C., Aronovitz, M.J., Iovanna, J.L., Patten, R.D., Kyriakis, J.M., and Goruppi, S. (2010). Deficiency of the transcriptional regulator p8 results in increased autophagy and apoptosis, and causes impaired heart function. Mol. Biol. Cell *21*, 1335–1349.

Kuma, A., Hatano, M., Matsui, M., Yamamoto, A., Nakaya, H., Yoshimori, T., Ohsumi, Y., Tokuhisa, T., and Mizushima, N. (2004). The role of autophagy during the early neonatal starvation period. Nature *432*, 1032–1036.

Lapierre, L.R., Kumsta, C., Sandri, M., Ballabio, A., and Hansen, M. (2015). Transcriptional and epigenetic regulation of autophagy in aging. Autophagy *11*, 867–880.

Levine, B., and Kroemer, G. (2008). Autophagy in the pathogenesis of disease. Cell *132*, 27–42.

Lisanti, M.P., Martinez-Outschoorn, U.E., Chiavarina, B., Pavlides, S., Whitaker-Menezes, D., Tsirigos, A., Witkiewicz, A., Lin, Z., Balliet, R., Howell, A., and Sotgia, F. (2010). Understanding the "lethal" drivers of tumor-stroma co-evolution: emerging role(s) for hypoxia, oxidative stress and autophagy/mitophagy in the tumor micro-environment. Cancer Biol. Ther. *10*, 537–542.

Martinez-Outschoorn, U.E., Trimmer, C., Lin, Z., Whitaker-Menezes, D., Chiavarina, B., Zhou, J., Wang, C., Pavlides, S., Martinez-Cantarin, M.P., Capozza, F., et al. (2010). Autophagy in cancer associated fibroblasts promotes tumor cell survival: role of hypoxia, HIF1 induction and NFκB activation in the tumor stromal microenvironment. Cell Cycle *9*, 3515–3533.

Martinez-Outschoorn, U.E., Pavlides, S., Howell, A., Pestell, R.G., Tanowitz, H.B., Sotgia, F., and Lisanti, M.P. (2011). Stromal-epithelial metabolic coupling in cancer: integrating autophagy and metabolism in the tumor microenvironment. Int. J. Biochem. Cell Biol. *43*, 1045–1051.

Martinez-Outschoorn, U.E., Peiris-Pagés, M., Pestell, R.G., Sotgia, F., and Lisanti, M.P. (2017). Cancer metabolism: a therapeutic perspective. Nat. Rev. Clin. Oncol. *14*, 11–31.

Menietti, E., Xu, X., Ostano, P., Joseph, J.M., Lefort, K., and Dotto, G.P. (2016). Negative control of CSL gene transcription by stress/DNA damage response and p53. Cell Cycle *15*, 1767–1778.

Mizushima, N., and Komatsu, M. (2011). Autophagy: renovation of cells and tissues. Cell *147*, 728–741.

Moscat, J., and Diaz-Meco, M.T. (2009). p62 at the crossroads of autophagy, apoptosis, and cancer. Cell *137*, 1001–1004.

Pavlides, S., Tsirigos, A., Migneco, G., Whitaker-Menezes, D., Chiavarina, B., Flomenberg, N., Frank, P.G., Casimiro, M.C., Wang, C., Pestell, R.G., et al. (2010). The autophagic tumor stroma model of cancer: role of oxidative stress and ketone production in fueling tumor cell metabolism. Cell Cycle *9*, 3485–3505.

Pietrocola, F., Izzo, V., Niso-Santano, M., Vacchelli, E., Galluzzi, L., Maiuri, M.C., and Kroemer, G. (2013). Regulation of autophagy by stress-responsive transcription factors. Semin. Cancer Biol. *23*, 310–322.

Procopio, M.G., Laszlo, C., Al Labban, D., Kim, D.E., Bordignon, P., Jo, S.H., Goruppi, S., Menietti, E., Ostano, P., Ala, U., et al. (2015). Combined CSL and p53 downregulation promotes cancer-associated fibroblast activation. Nat. Cell Biol. *17*, 1193–1204.

Ratovitski, E.A. (2011). ΔNp63α/IRF6 interplay activates NOS2 transcription and induces autophagy upon tobacco exposure. Arch. Biochem. Biophys. *506*, 208–215.

Sample, A., Zhao, B., Qiang, L., and He, Y.Y. (2017). Adaptor protein p62 promotes skin tumor growth and metastasis and is induced by UVA radiation. J. Biol. Chem. *292*, 14786–14795.

Söderberg, O., Gullberg, M., Jarvius, M., Ridderstråle, K., Leuchowius, K.J., Jarvius, J., Wester, K., Hydbring, P., Bahram, F., Larsson, L.G., and Landegren, U. (2006). Direct observation of individual endogenous protein complexes *in situ* by proximity ligation. Nat. Methods *3*, 995–1000.

Valencia, T., Kim, J.Y., Abu-Baker, S., Moscat-Pardos, J., Ahn, C.S., Reina-Campos, M., Duran, A., Castilla, E.A., Metallo, C.M., Diaz-Meco, M.T., and Moscat, J. (2014). Metabolic reprogramming of stromal fibroblasts through p62-mTORC1 signaling promotes inflammation and tumorigenesis. Cancer Cell *26*, 121–135.

White, E. (2015). The role for autophagy in cancer. J. Clin. Invest. *125*, 42–46.

Zhao, X., He, Y., and Chen, H. (2013). Autophagic tumor stroma: mechanisms and roles in tumor growth and progression. Int. J. Cancer *132*, 1–8.

STAR★METHODS

KEY RESOURCES TABLE

REAGENT or RESOURCE	SOURCE	IDENTIFIER
Antibodies		
Rabbit monoclonal anti CSL	Cell Signaling	Cat# 5313; AB_2665555
Rabbit monoclonal anti LC3B	Cell Signaling	Cat# 3868; AB_2137707
Rabbit monoclonal anti β-ACTIN	Cell Signaling	Cat# 5125; AB_1903890
Rabbit monoclonal anti SQSTSM/p62	Sigma	Cat# P0067; AB_1841064
Rabbit anti CSL	Procopio et al., 2015	N/A
Rabbit anti GFP	Santa Cruz	Cat# 8334; AB_641123
Rabbit anti ATG5	Epitomics	Cat# 3167-1; N/A
Mouse monoclonal anti SQSTSM/p62	Santa Cruz	Cat# 28359; AB_628279
Mouse monoclonal anti FLAG	Sigma-Aldrich	Cat# F3165; AB_259529
Mouse monoclonal anti GAPDH	Santa Cruz	Cat# 47724; AB_627678
Biological Samples		
HDFs: discarded skin samples of abdominoplasty patients at Massachusetts General Hospital	Dermatology, MGH, Boston, MA	N/A
CAFs: surgically excised discarded skin SCC samples	Dermatology, MGH, Boston, MA	N/A
Chemicals, Peptides, and Recombinant Proteins		
Recombinant human CSL	Origene	Cat# TP760429
Recombinant human p62	Enzo	Cat# ENZ-PRT120-0050
Bafilomycin A1	EMD Millipore	Cat# 19-149
3-methyladenine	Sigma-Aldrich	Cat# M9281-100MG
mTOR inhibitor KU0063794	Calbiochem	Cat# CAS 938440-64-3
Carbonyl cyanide m-chloro-phenyl-hydrazone (CCCP)	Calbiochem	Cat# CAS 555-60-2
Puromycin	Calbiochem	Cat# CAS 58-58-2
Doxycycline	Calbiochem	Cat# CAS 24-390-14-5
Hiperfect	Quiagene	Cat# 301707
Lipofectamine 2000	Invitrogene	Cat# 11668019
Liberase TL	Roche	Cat# 5401020001
Flag-MAGNETIC beads	Sigma-Aldrich	Cat# M8823-1ML
Donkey anti rabbit peroxidase conjugated	Thermo Fisher	Cat# NA934V
Donkey anti mouse peroxidase conjugated	Thermo Fisher	Cat# NA931V
Donkey anti rabbit Alexa 488	Invitrogen	Cat# A 21206
Phalloidin RITC	Sigma-Aldrich	Cat# P1951-1MG
Critical Commercial Assays		
Proximity ligation assay - Duolink	Sigma-Aldrich	Cat# DUO92101
Experimental Models: Cell Lines		
MEFs Atg5 +/+	Kuma et al., 2004	N/A
MEFs Atg5 −/−	Kuma et al., 2004	N/A
MEFs p62 +/+	Komatsu et al., 2006	N/A
MEFs p62 −/−	Komatsu et al., 2006	N/A
HEK293	ATCC	RRID: SCR_001672
Human primary dermal fibroblasts	This paper	SAN1
Human primary dermal fibroblasts	This paper	SAN2
Human primary dermal fibroblasts	This paper	SAN3
Human primary dermal fibroblasts	This paper	SAN4

(*Continued on next page*)

Continued

REAGENT or RESOURCE	SOURCE	IDENTIFIER
Human primary dermal fibroblasts	This paper	SAN5
Human primary dermal fibroblasts	This paper	SAN6
Human primary dermal fibroblasts	This paper	SAN8
Human cancer associated fibroblasts	This paper	CAF1
Human cancer associated fibroblasts	This paper	CAF2
Human cancer associated fibroblasts	This paper	CAF3
Human cancer associated fibroblasts	This paper	CAF4
Human cancer associated fibroblasts	This paper	CAF16
Oligonucleotides		
siRNA scrambled control -Silencer	Ambion	Cat# 4390846; ID: N/A
siRNA targeting p62 -Silencer	Ambion	Cat# 4427037; ID: 16962
siRNA targeting CSL -Silencer	Ambion	Cat# 4392420; ID 24886
shRNA empty control N/A	Sigma-Aldrich	pLKO_TRC001
shRNA targeting p62 CCGGCCCTTTGTCTTGTAGTTGCAT CTCGAGATGCAACTACAAGACAAAGGGTTTTTG	Sigma-Aldrich	TRCN0000098615
shRNA targeting ATG5 CCGGGCCAAGTATCTGTCTATGA TACTCGAGTATCATAGACAGATACTTGGCTTTTTG	Sigma-Aldrich	TRCN0000099430
Oligonucleotides for PCR are listed in Table S1		
Recombinant DNA		
GFP-p62	Bjørkøy et al., 2005	N/A
GFP-p62 ΔPB1	Bjørkøy et al., 2005	N/A
GFP-p62 ΔUBA	Bjørkøy et al., 2005	N/A
GFP-p62 ΔLIR	Bjørkøy et al., 2005	N/A
CSL-FLAG	Procopio et al., 2015	N/A
Myc-CSL inducible	Procopio et al., 2015	N/A
Software and Algorithms		
IMAGEJ	NIH	https://imagej.nih.gov/ij/
Prism 7	Graphpad software	https://www.graphpad.com

CONTACT FOR REAGENT AND RESOURCE SHARING

Further information and requests for resources and reagents should be directed to and will be fulfilled by the Lead Contact Gian Paolo Dotto (paolo.dotto@unil.ch)

EXPERIMENTAL MODEL AND SUBJECT DETAILS

Human samples

Normal human skin samples and samples of squamous cell carcinoma (SCC) were obtained at the Department of Dermatology, Massachusetts General Hospital, as discarded parts not needed for diagnosis. All samples were processed as approved by the MGH Institutional Review Board. The age/stage, sex and gender identity of the subjects was not available.

Cell culture and primary cell derivation

All the cells were routinely grown at 37 in a 5% CO2 incubator in DMEM Cellgro#15-017CV, 10%FBS, 2mM Glutamine and 100U/ml penicillin, 100μg streptomycin. All cellular strains used were routinely checked for the absence of mycoplasma.

Normal HDFs were prepared from discarded skin samples of abdominoplasty patients at Massachusetts General Hospital (Boston, Massachusetts, USA) as in (Procopio et al., 2015). Each HDF strain was identified by letters recognizing the operator and a number, which are indicated in the different panels and listed in the Key Resources Table. For derivation of cancer associated fibroblasts (CAFs), surgically excised discarded skin SCC samples were dissociated with Liberase TL (Roche) as in (Goruppi et al., 2017). The isolated CAFs strains were validated in immunofluorescence as vimentin positive and pan Keratin negative. Each strain derived from

a patient was identified with a progressive number, which is indicated in the different panels and listed in Key Resources Table. The information on sex/gender/age was not available.

METHOD DETAILS

Cell manipulation

RNA-mediated gene interference experiments were carried out with Silencer™ siRNA oligos from Ambion and Hiperfect reagents (QIAGEN) (for *CSL* and *p62*), or, by using shRNA gene targeting lentiviral vectors from Sigma Aldrich (for *p62* and *ATG5),* as previously described (Goruppi et al., 2017; Procopio et al., 2015). The lentiviral vectors (in the pLKO.1 backbone) were packaged using PEI (Sigma) in actively growing 293 HEK cells in combination with pMD2.G/ /Rev/RRE plasmids. Virus containing supernatants were collected 72h from transfection filtered to eliminate cell particulates and used to infect HDFs or MEFs in the presence of 10μg polybrene (Millipore). Cells were subsequently used for the experiments after puromycin selection (1μg/ml) for 48-72 h.

HDFs strains stably infected with a doxycycline-inducible lentiviral vector for Myc-tagged CSL in parallel with empty vector control (Procopio et al., 2015) were treated for 3 days plus/minus doxycycline (200 ng ml^{-1}) before autophagy induction for 24h and analysis.

The list of the antibodies, reagents, cell lines, MEFs, HDFs, CAFs, siRNA and shRNA sequences used are in the Key Resources Table.

Gene Expression analysis

Conditions for reverse transcription and quantitative cDNA amplification (RT–qPCR**)** have been previously reported (Goruppi et al., 2017; Procopio et al., 2015). Total RNA was extracted using a Quiagene kit, and 750 ng reverse transcribed with iScript cDNA synthesis kit (BioRad). Quantitative amplification was performed with a Roche real-time thermocycler and the expression of the genes was normalized with BETA ACTIN. *The oligonucleotides used in qPCR are provided in* Table S1.

Autophagy studies, immunofluorescence and immunoblots

HDFs and MEFs autophagy was activated by incubating the cells in serum free or by adding to the culture medium (10%FBS) 10μM mTOR inhibitor KU0063794 (Calbiochem) or 100nM carbonyl cyanide m-chloro-phenyl-hydrazone (CCCP) mitochondrial uncoupling agent (Calbiochem) for 24h. Western blots and immunofluorescences were performed as in (Kong et al., 2010; Procopio et al., 2015).

Cells for protein analysis were washed in PBS ice cold then lysed in LDS-NuPAGE loading buffer 1x (Invitrogen) with phosphatase and protease inhibitors before separation of the total cell lysates on 4%–12% Bis-Tris gels (Invitrogen). Equal amount was loaded for each sample as assessed with separate Comassie blue stained gels and verified by sequential blotting of the same membrane with a control antibody (TUBULIN, ACTIN or GAPDH, as indicated). For immunofluorescence cells were counted with a haemocytometer and seeded on coverslips. The next day the HDFs or MEFs were treated as indicated to activate autophagy and thus fixed after 20 h with 3% PFA in PBS for the analysis. Phalloidin and DAPI were used to counterstain the cytoskeleton and the nucleus respectively. Slides were mounted with Fluomount-G (Southern Biotech) and analyzed using a Nikon Eclipse TE300 fluorescence microscope.

Immunoprecipitations and protein interaction

The co-immunoprecipitation of p62 and CSL was performed from HDFs using a native lysis buffer (150mM NaCl, 50mMTris pH7, 1% Triton X-100, 10mM PMSF and PIC, Roche), in the presence of 4μg of anti CSL or NRS (Cell Signaling) and 40 μl Protein G magnetic beads (Life Technologies) for 4h at 4C. The complexes were washed 4 times in lysis buffer and eluted with SDS-running buffer. For the interaction of CSL with p62 wt and deletion constructs, 3μg of CSL-Flag and 3μg of GFP tagged wild-type, ΔPB1, ΔUBA and ΔLIR region (Bjørkøy et al., 2005) were transfected in 293 cells using PEI method. After 48h the cells were lysed in native lysis and the immunoprecipitation carried out using 40μl Flag-MAGNETIC beads (Sigma). The complexes were washed 5 times in lysis buffer before the sequential immunoblotting with GFP (Santa Cruz) and Flag M2 (Sigma) antibodies.

For the recombinant protein interaction, 500 ng of recombinant CSL (Origene) and p62 (Enzo) were diluted in 500 μl PBS and incubated 2h at 4C on a rotor. The sample was split in two for over night incubation with 1μg of specific antibody against CSL (Cell Signaling) or p62 (Sigma) and non-specific rabbit IgG respectively, as control. 25 μl Dynabeads (Invitrogen) were added for additional 4h at 4°C with rotation. Bait and prey were immunoprecipitated using a magnet and washed 4 times with 500 μl PBS before boiling with sample buffer and western blotting.

Proximity ligation assays (Söderberg et al., 2006) were performed using Duolink PLA kit (Sigma) according to manufacturer's protocol. Briefly, cells were fixed with 4% formaldehyde and permeabilized in 0.1% Triton X-100. After blocking with PLA blocking solution, HDFs were incubated with primary antibody solution containing p62 (Santa Cruz) and CSL (Cell Signaling) antibodies (both from Santa Cruz). After washing with PLA wash buffer, cells were incubated with PLA probes, anti-rabbit PLUS, anti-mouse MINUS, then washed, ligated, amplified by rolling circle amplification. Images were obtained with a Nikon Eclipse Ti confocal microscope.

QUANTIFICATION AND STATISTICAL ANALYSIS

Data are presented as mean ± SEM, mean ± SD, or as ratio among treated and controls, as indicated in the Figure legends. For gene expression and functional testing assays, statistical significance of differences between experimental groups and controls was assessed by two-tailed unpaired t test, as indicated in the figure legends. A value for $p < 0.05$ was considered as statistically significant. For each experiment, two to three separate HDF strains were used in independent experiments. The CAFs from four independent patients were used. The researchers were not blinded and no strain or result was excluded from the analysis.

DATA AND SOFTWARE AVAILABILITY

Unprocessed original image data have been deposited to Mendeley Data and are available at https://doi.org/10.17632/grw7vdjkdb.1.